北見工業大学研究報告
第18巻 第1号 (昭和61年)

Memoirs of the Kitami Institute of Technology
Vol. 18 No. 1 (1986)

Loci of Forced Cycling Operation and Transient Chemical Oscillation in Heterogeneous Catalysis*

by Tohru KANNO**, Hatsuo TANAKA*** and Masayoshi KOBAYASHI**

(Received April 24, 1986)

Abstract

A mathematical model to analyse the forced cycling response and the self oscillation in heterogeneous catalysis is proposed for a tubular flow reactor, and a computer simulation technique is applied to evaluate the validity of the model proposed. A typical E-R model reaction and hydrogen oxidation on a thin nickel foil are employed as a concrete subject. When the stimulus of the sine-function and the step function of reactants are introduced into the differential reactor, the mode of the response curves of products at the outlet of the reactor is sensitively affected by the desorption rate of the products. It is exactly confirmed that the reactor efficiency to produce the objective products is not affected by the forced concentration cyclic operation.

Slinko's model for the computer simulation is satisfactorily applied to visualize the self oscillation resulting from the change in the rate constants which vary with the surface coverage of the adsorbed species. The concentration of the reactants and the exponential factors of rate constants have a drastic effect on the appearance of oscillation restricted by the specified ranges of their magnitude. The locus of the transient oscillation caused by the concentration jump is clearly displayed and characterized depending on the amplitudes and the frequencies.

1. Introduction

Considerable oscillating behavior in heterogeneous catalytic reaction has been reported in much broader systems, such as reactor multiplicity, steady state multiplicity of reaction and chemical oscillation in heterogeneous catalysis. Recently, the chemical oscillation in heterogeneous catalysis has increasingly been scrutinized because of the fast progress and the development of new instruments to analyse the surface structure of solids under in situ conditions.

For the oscillation in catalytic reactions, several explanations have been presented; (1) a shift in the form of adsorbed species between two different forms,[6] (2) oscillations in the concentration of reactants in the pores of supports caused by the diffusion rate limitation[7~9], (3) change in the reaction route with the surface coverage of reactants[9], (4) fluctuations in the surface coverage of a

* The paper was presented at the Hokkaido regional meeting of the Chemical Society of Japan in the winter period of 1980.

** Department of Industrial Chemistry, Kitami Institute of Technloogy.
*** Nihon-Data Skill Co.

specified impurity,[10] (5) cyclic changes in the oxidation state of metal oxides[11] and (6) changes in the rate constants of reaction sequence with the surface coverage of reactants.[12]

Recently, three evidences have been found to explain the oscillation : (1) a shift between two different phases,[13,14] (2) lattice compression by adsorbed species[15] and (3) a shift between the oxidation and the reduction states of the catalyst surface.[16]

In the present study, four subjects have been taken : (1) the presentation of a mathematical model to describe the reactor response caused by the forced cycling change in the concentration of reactants, (2) the possibility of an efficiency increase to form the products due to the cyclic operations, (3) the computer simulation of chemical oscillation in the oxidation of H_2 on a nickel foil as an example and (4) parameter sensitivities of rate constants and the concentration of reactants to the oscillating responses. For the computer simulation of chemical oscillation, Slinko's model is chosen taking into account the change in the rate constants caused by the shift of surface state between two different structures. Based on the model, the mathematical expressions to estimate the forced cycling response and the oscillation behavior are proposed, and the parameter sensitivities to the cycling behavior and the oscillation behavior have also been studied in detail.

For the computer simulation, three commercial personal computers (PC 8001 mk II (NEC)) are simultaneously used, and the results obtained are monitored by an X-Y plotter (Rikadenki RY-20).

2. Transient Behavior of Forced Cycling Operation

2-1. Model Description

A model reaction is proposed to analyse the transient behavior of the forced cycling operation :

$$X_1(g)+S \underset{k_{-1}}{\overset{k_1}{\rightleftharpoons}} X_1 \cdot S \qquad (1)$$

$$X_1 \cdot S + X_2(g) \xrightarrow{k_2} Y \cdot S \qquad (2)$$

$$Y \cdot S \underset{k_{-3}}{\overset{k_3}{\rightleftharpoons}} Y(g)+S \qquad (3)$$

which is an Eley-Rideal mechanism.

A tubular flow reactor for the reaction is used and the reaction conditions are chosen so as to satisfy a differential reactor, in which the total conversion of reactants should be less than 10%. One therefore can presume the averaged concentration of reaction components to be half the concentration at the outlet. The reactor parameters used are presented in Table 1.

The basic material balance equations are derived at the gas phase and the adsorbed phase. The differential volume is taken in a tubular reactor by a

Table 1. The reactor parameters used for the computer simulation of forced cycling oscillation

Reactor length	$L = 100$ (cm)
Superficial gas velocity	$U = 400$ (cm/min)
Saturated amount of adsorbed species i	$q_i = 0.1\times10^{-3}$ (mol/g)
Void fraction of packed bed reactor	$\varepsilon = 0.5$ (−)
Catalyst bed density	$\rho_c = 1$ (g/cm^3)
Reaction temperature	$T = 373$ (K)

circular disk of differential thickness dZ. In the differential element, AdZ, reactant X is introduced by flow and removed by flow and chemical reaction. The flow rate, if any, will be changed by the volume change due to chemical reaction. For reactant X, the equations may be derived with all terms having units of moles of X per minute:

$$\text{Input by flow} = \frac{UA\rho_M P_{X_1}}{\pi} \tag{4}$$

$$\text{Output by flow} = \frac{A\rho_M}{\pi}\left(P_{X_1} + \frac{\partial P_{X_1}}{\partial Z}dZ\right)\left(U + \frac{\partial U}{\partial Z}dZ\right) \tag{5}$$

$$\text{Output by chemical reaction} = (k_1 P_{X_1}\theta_V - k_{-1}\theta_{X_1})\,\rho_C A dZ \tag{6}$$

$$\text{Accumulation} = \rho_M \frac{\varepsilon}{\pi} A(\partial P_{X_1}/\partial t)\,dZ \tag{7}$$

where $\rho_M = \pi/RT$

The material balance leads us to input minus output equals accumulation and thereby the following equation may be derived:

$$\frac{-1}{\rho_C RT}\left(U\frac{\partial P_{X_1}}{\partial Z} + P_{X_1}\frac{\partial U}{\partial Z}\right) - (k_1 P_{X_1}\theta_V - k_{-1}\theta_{X_1}) = \frac{\varepsilon}{\rho_C RT}\frac{\partial P_{X_1}}{\partial t} \tag{8}$$

Here, the superficial gas velocity, U, will be changed along the reactor length by the changes in temperature, pressure and total molar flow rate caused by the progress of the reaction. In this work, the differential reactor is chosen and therefore, the change in the total molar flow rate may be negligibly small. In addition, the change in the temperature and pressure may also be negligible because of its mild reaction conditions and well controlled systems. Considering these assumptions, Equation (8) becomes

$$\frac{\partial P_{X_1}}{\partial t} = \frac{-U}{\varepsilon}\frac{\partial P_{X_1}}{\partial Z} - \frac{\rho_C RT}{\varepsilon}(k_1 P_{X_1}\theta_V - k_{-1}\theta_{X_1}) \tag{9}$$

Similar derivations are carried out for the gas phase and the adsorbed phase, and we obtain

$$\frac{\partial P_{X_2}}{\partial t} = \frac{-U}{\varepsilon}\frac{\partial P_{X_2}}{\partial Z} - \frac{\rho_C RT}{\varepsilon}k_2 P_{X_2}\theta_{X_1} \tag{10}$$

$$\frac{\partial P_Y}{\partial t}=\frac{-U}{\varepsilon}\frac{\partial P_Y}{\partial Z}-\frac{\rho_C RT}{\varepsilon}k_3\theta_Y \tag{11}$$

$$\frac{\partial \theta_{X_1}}{\partial t}=\frac{1}{q_m}(k_1P_{X_1}\theta_V-k_{-1}\theta_{X_1}-k_2P_{X_2}\theta_{X_1}) \tag{12}$$

$$\frac{\partial \theta_Y}{\partial t}=\frac{1}{q_m}(k_2P_{X_2}\theta_{X_1}-k_3\theta_Y+k_{-3}P_Y\theta_V) \tag{13}$$

Noting the differential reactor, one may use an arithmetic average for the concentration in the reactor, and the partial differential equations obtained above may be rewritten by ordinary differential equations. For product Y, one may express

$$\frac{d}{dt}\frac{P_Y^0+P_Y}{2}=\frac{U}{\varepsilon}\frac{P_Y^0-P_Y}{L}-\frac{\rho_C RT}{\varepsilon}\left\{k_{-3}\left(\frac{P_Y^0+P_Y}{2}\right)\theta_V-k_3\theta_Y\right\} \tag{14}$$

Equation (14) may be rewritten by

$$\frac{dP_Y}{dt}=\frac{-2U}{\varepsilon L}P_Y+\frac{2\rho_C RT}{\varepsilon}\left(k_3\theta_Y-\frac{k_{-3}P_Y\theta_V}{2}\right) \tag{15}$$

Similar procedures are applied for other components.
The equations for the gas phase are

$$\frac{dP_X}{dt}=\frac{U}{\varepsilon L}(P_{X_1}^0-P_{X_1})-\frac{\rho_C RT}{\varepsilon}k_1P_{X_1}\theta_V \tag{16}$$

and for the adsorbed phase,

$$\frac{d_{X_1}}{dt}=\frac{1}{q_m}(k_1P_{X_1}\theta_V-k_{-1}\theta_{X_1}-k_{-2}P_{X_2}\theta_{X_1}) \tag{17}$$

$$\frac{d\theta_Y}{dt}=\frac{1}{q_m}(k_2\theta_{X_1}\theta_{X_2}-k_3\theta_Y+k_{-3}P_Y\theta_V) \tag{18}$$

$$\theta_V=1-\theta_X-\theta_Y \tag{19}$$

2-2. Forced Frequency Concentration Cycling Operation

(1) Presentation of Basic Equations

One may propose an input forcing function by

$$P_{X_i}=P_{X_i}^0\{1+M\sin(2\pi t/N)\} \tag{20}$$

In Equation (20), the partial pressure of X_2 at the inlet of the reactor is $P_{X_2}=0$ atm at $t=0$ and can be varied by the amplitude of M and the period of N min as a function of the elapsed time. To simulate the transient response curves caused by the forced cyclic concentration change operation, equations (14)-(19) should simultaneously be solved.

(2) Parameters Affecting the Response Curves

In our previous papers, the mode of the transient response curves caused by the concentration jump is drastically affected by the reaction mechanism and the modes are classified into six typical types[17]. Two characteristic modes are chosen

to simulate the forced cycling response curves; (1) a monotonic mode (type II) which is characterized by the two-step rate controlling mechanism, the surface reaction and the desorption of products, and (2) an overshoot mode (type IV) which is characterized by the slow regeneration of active sites or active species.

Fig. 1 illustrates a typical transient response curve based on the two-step controlling mechanism, and the kinetic parameters used are presented in the figure. After the catalyst is treated by an X_1 (20%)-inert gas mixture to make the surface coverage of 1.0, an X_1-X_2 mixture is introduced into the reactor and the response of product Y is followed for 70 min. The response of Y (curve II) completes a steady state up to 40 minutes, indicating a typical monotonic mode (type II). At 70 min, the concentration of X_1 (curve I) is continuously changed by a forced function with the amplitude of $M=0.3$ atm and the period of $N=22$ min using Equation (20). Comparing curves II with I in Run 3, one may recognize the effect as reducing the amplitude by about 30% with a little change in the period. This reducing effect should result from the slow desorption of Y, even though k_3 is larger than k_2.

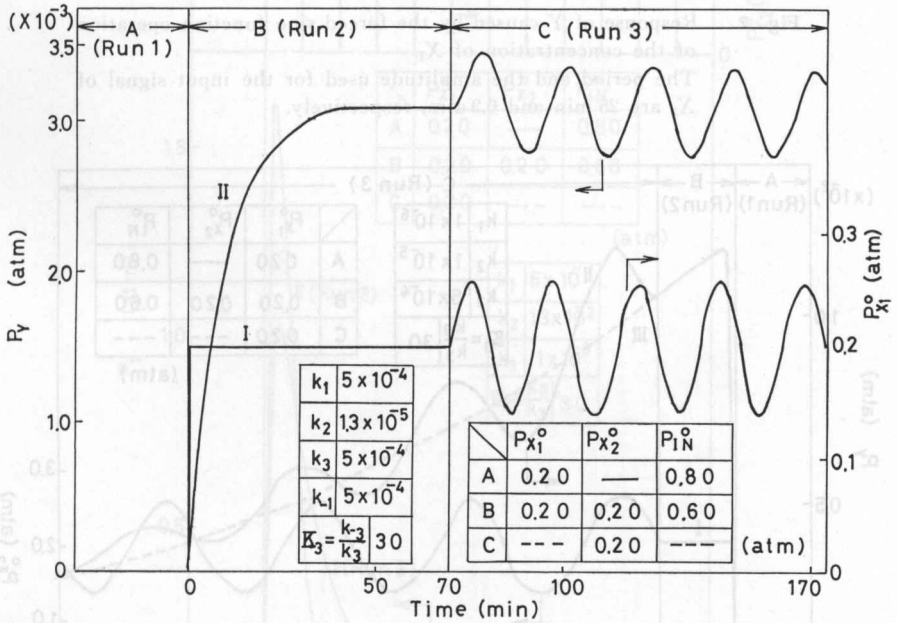

Fig. 1. Response of Y caused by the forced sine function operation of the concentration of X_1.
The period and the amplitude used for the input signal of X_1 are 22 min and 0.3 atm, respectively.

When the desorption of Y is a rate determining step, the response of Y indicates little change in the concentration as shown in Fig. 2 by curve II (Run 3). Although the amplitude is greatly reduced, in this case, the period again shows no change with $N=25$ min. Based on the above discussions, one may

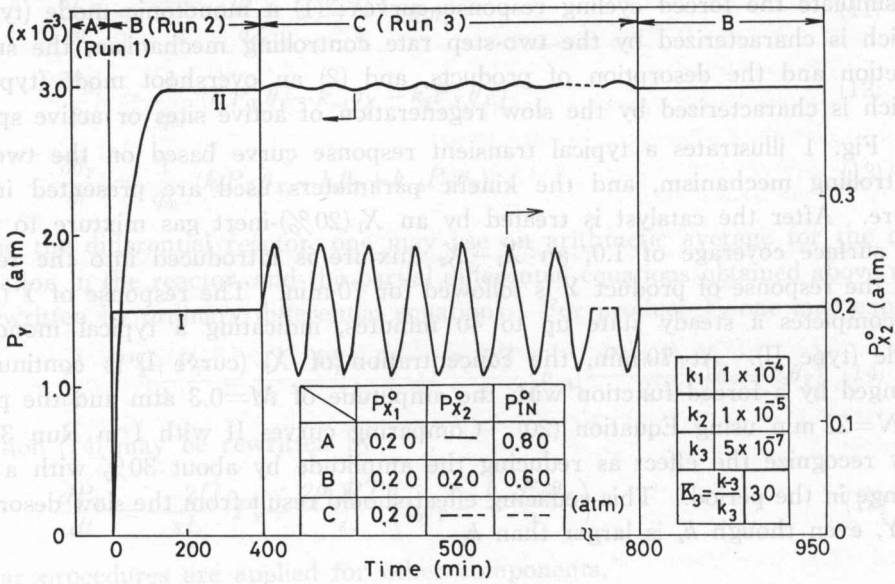

Fig. 2. Response of Y caused by the forced sine function operation of the concentration of X_1.
The period and the amplitude used for the input signal of X_2 are 25 min and 0.3 atm, respectively.

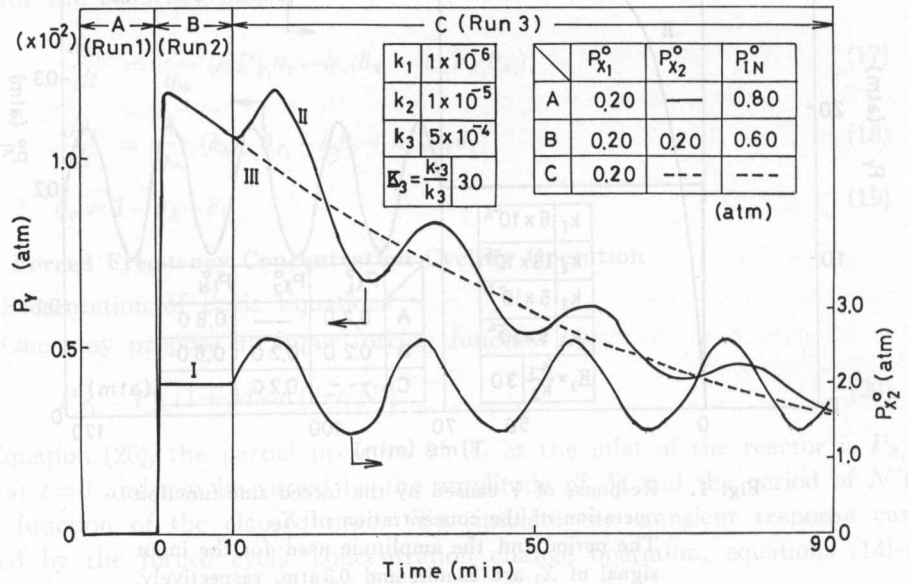

Fig. 3. Comparison of the responses of Y caused by the step increase of X_2 (Curve IV) and the forced sine function operation of X_2 (Curve II). Curve I shows an input sine function for Curve II.
The period and the amplitude used for the input signal of X_2 are 25 min and 0.3 atm, respectively.

conclude that the amplitude of the forced response curve is affected by the desorption rate constants of the product, whereas the period is not influenced.

Fig. 3 illustrates a forced frequency response based on the mechanism controlled by regeneration of the active adsorbed species (type IV). The X_2 (inc., 0) $-$ Y response is followed for ten minutes (Run 2) and then two different simulations are separately conducted (Run 3): (1) the forced frequency response is successively followed for 80 min (curve II), and (2) the X_2 (inc., 0) $-$ Y response is continued as such for 90 min (curve III). Curve II oscillates around curve III while gradually decreasing its amplitude. As can be seen from the response curves, the overshoot tendency is not affected by the forced cycling feed. In addition, the graphical integrations of curves II and III are carried out up to 90 min and then compared, and found to show a good agreement indicating no change in the yield of Y by the cyclic operation.

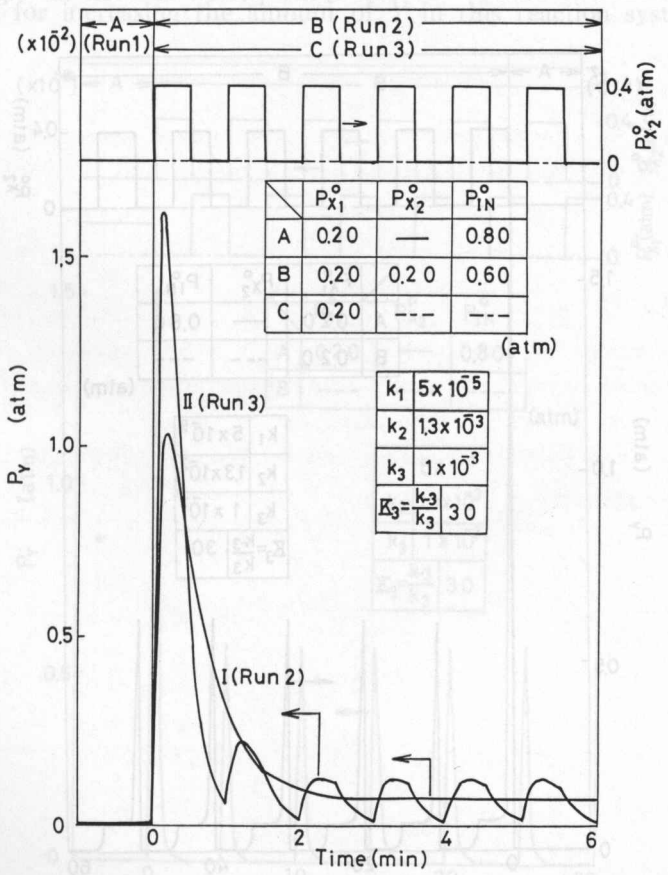

Fig. 4. Comparison of the responses of Y caused by the step function of X_2 (Curve I) and the forced rectangular cyclic operation of X_2 (Curve II).
The period and the amplitude used for the input signal of X_2 are 30 sec and 0.2 atm, respectively.

2-3. Forced Rectangular Concentration Cycling Operation

The transient response of Y caused by the step increase of X_2 is simulated using a reactor length of 1 cm, and the result is represented in Fig. 4 by curve I. The response is completed within three minutes, and differing from the curve III in Fig. 3, for three reasons: (1) k_2 and k_3 in Fig. 4 are two orders higher than those in Fig. 3, (2) the reaction is controlled only by the adsorption of X_1 and (3) the reactor length is one hundred times shorter than the previous one.

Curve II in Fig. 4 illustrates the response of Y caused by the rectangular forced concentration cycling operation of X_2. The cycling period is 30 sec. The response in the first period is extremely different from the others, resulting from the surface coverage of Y, θ_Y, which is equal to one at the initial stage of the first period, whereas periods other than the first period have a very low value of θ_Y. The shape of all the response curves clearly exhibits an overshoot type. When five minutes is chosen for the cyclic period as seen in Fig. 5 using the

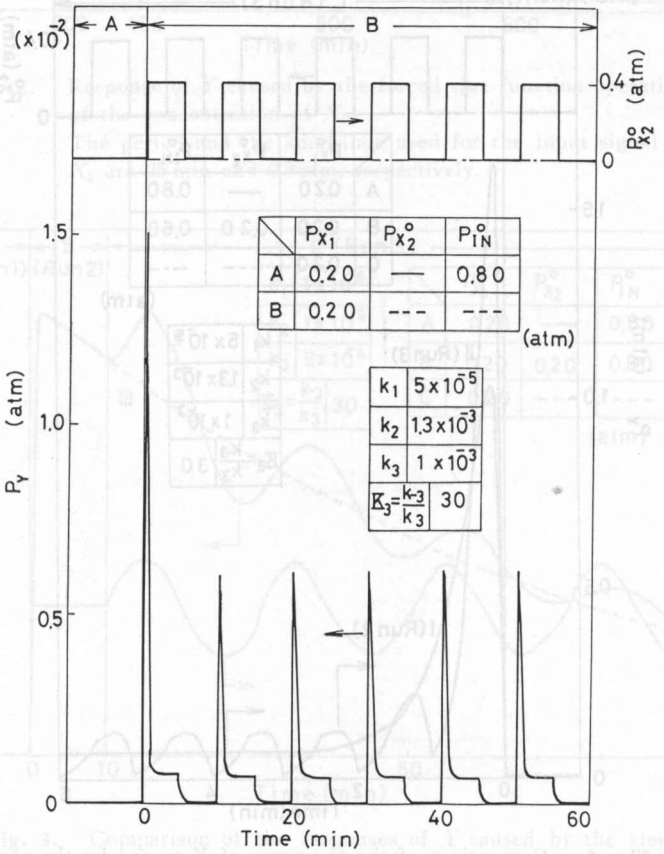

Fig. 5. Response of Y caused by the forced rectangular cyclic operation of X_2.
The period and the amplitude used for the input signal are 5 min and 0.2 atm, respectively.

same k_j as in Fig. 4, then the response is completed within about five minutes and shows the same mode as periods other than the first period.

Fig. 6 illustrates the response curves of Y caused by the simultaneous opposite cyclic change in the concentration of X_1 with X_2. The X_1, X_2–Y response curve shows a steep shape with a peak, which is due to the slow regeneration of adsorbed X_1. The graphical integration of the response curve in the first period gives the saturated amount of adsorbed X_1 and estimates to be 0.1×10^{-3} (mol/g) ($\theta_{X_1}=1.0$). The graphical integration of the response curves other than the first period gives a surface coverage of X_1 adsorbed within 2.5 min, and θ_{X_1} is evaluated to be about 0.4.

Noting the change in the yield of Y, one may integrate curves I and II in Fig. 4 up to 6 min and compare the integrated amounts, 1.81×10^{-6} and 1.84×10^{-6} mol/g. There is no appreciable difference between them. This clearly indicates that the cyclic operation due to the forced rectangular function is not very effective for increasing the amount of Y in this reaction system.

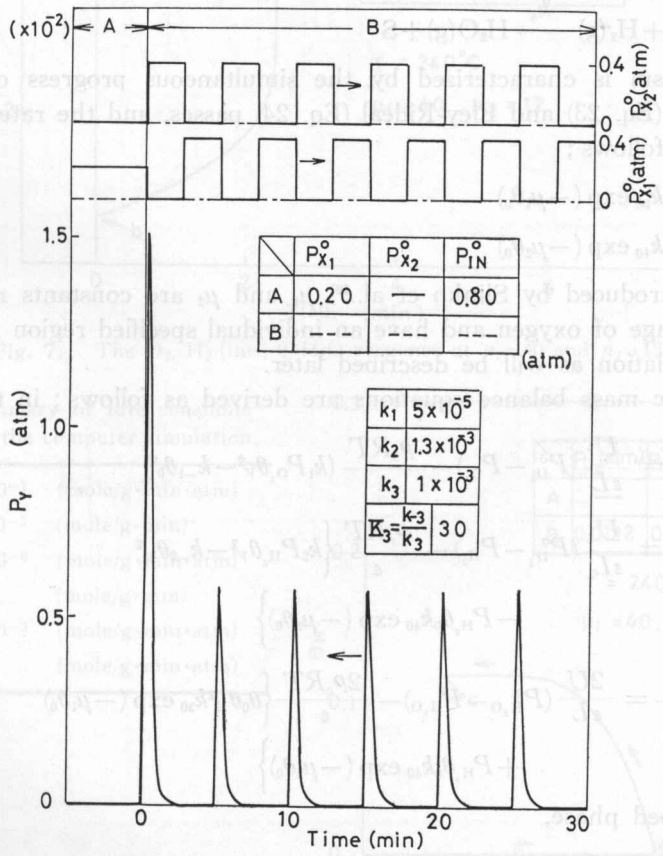

Fig. 6. Response of Y caused by the simultaneous forced rectangular cyclic operation of X_1 and X_2.
The period and the amplitude are 2.5 min and 0.2 atm for X_1 and X_2, respectively.

3. Transient Behavior of Self Oscillation

3-1. Presentation of Reaction Model and Material Balance Equations

Belyaev, M. M. Slinko and M. G. Slinko[18] have studied the oxidation of hydrogen on a nickel foil at temperatures ranging from 150 to 300°C and found the typical oscillation behavior. Based on their experimental results and those proposed by other researchers, the following mechanism may be considered;

$$O_2+2S \underset{k_{-1}}{\overset{k_1}{\rightleftharpoons}} 2O\cdot S \tag{21}$$

$$H_2+2S \underset{k_{-2}}{\overset{k_2}{\rightleftharpoons}} 2H\cdot S \tag{22}$$

$$O\cdot S+2H\cdot S \xrightarrow{k_3} H_2O(g)+3S \tag{23}$$

$$O\cdot S+H_2(g) \xrightarrow{k_4} H_2O(g)+S \tag{24}$$

The mechanism is characterized by the simultaneous progress of Langumuir-Hinshelwood (Eq. 23) and Eley-Rideal (Eq. 24) passes, and the rate constants are expressed as follows;

$$k_3 = k_{30}\exp(-\mu_1\theta_0) \tag{25}$$

$$k_4 = k_{40}\exp(-\mu_2\theta_0) \tag{26}$$

which are introduced by Slinko et al..[19] μ_1 and μ_2 are constants relating to the surface coverage of oxygen and have an individual specified region for the appearance of oscillation as will be described later.

The basic mass balance equations are derived as follows; in the gas phase,

$$\frac{dP_{O_2}}{dt} = \frac{U}{\varepsilon L}(P^0_{O_2}-P_{O_2}) - \frac{\rho_c RT}{\varepsilon}(k_1 P_{O_2}\theta_V^2 - k_{-1}\theta_0^2) \tag{27}$$

$$\frac{dP_{H_2}}{dt} = \frac{U}{\varepsilon L}(P^0_{H_2}-P_{H_2}) - \frac{\rho_c RT}{\varepsilon}\Big\{k_2 P_{H_2}\theta_V^2 - k_{-2}\theta_H^2 - P_{H_2}\theta_0 k_{40}\exp(-\mu_2\theta_0)\Big\} \tag{28}$$

$$\frac{dP_{H_2O}}{dt} = \frac{2U}{\varepsilon L}(P^0_{H_2O}-P_{H_2O}) - \frac{2\rho_c RT}{\varepsilon}\Big\{\theta_0\theta_H^2 k_{30}\exp(-\mu_1\theta_0) + P_{H_2}\theta_0 k_{40}\exp(-\mu_2\theta_0)\Big\} \tag{29}$$

In the adsorbed phase,

$$\frac{d\theta_0}{dt} = \frac{1}{q_m}\Big\{2k_1 P_{O_2}\theta_V^2 - 2k_{-1}\theta_0^2 - \theta_0\theta_H^2 k_{30}\exp(-\mu_1\theta_0) - P_{H_2}\theta_0 k_{40}\exp(-\mu_2\theta_0)\Big\} \tag{30}$$

Table 2. The reactor parameters used for the computer simulation of self oscillation

Reactor length	$L=60$ (cm)
Superficial gas velocity	$U=30{,}000$ (cm/min)
Saturated amount of adsorbed species i	$q_i=1.95\times10^{-6}$ (mole/g)
Void fraction of packed bed reactor	$\varepsilon=9.997\times10^{-1}$ (—)
Catalyst bed density	$\rho_c=2.65\times10^{-3}$ (g/cm^3)

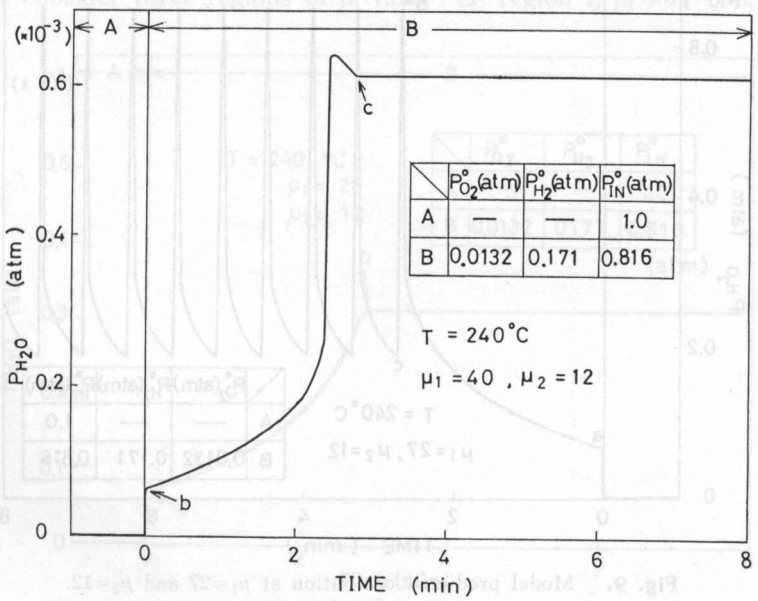

Fig. 7. The O_2, H_2 (inc., 0)-H_2O response at $\mu_1=40$ and $\mu_2=12$.

Table 3. Summary of rate constants for the computer simulation

$k_1 = 2.08\times10^{-1}$	(mole/g·min·atm)
$k_{-1}= 4.88\times10^{-3}$	(mole/g·min)
$k_2 = 1.28\times10^{-6}$	(mole/g·min·atm)
$k_{-2}= 0$	(mole/g·min)
$k_{30} = 4.54\times10^{-3}$	(mole/g·min·atm)
$k_{40} = 0.571$	(mole/g·min·atm)

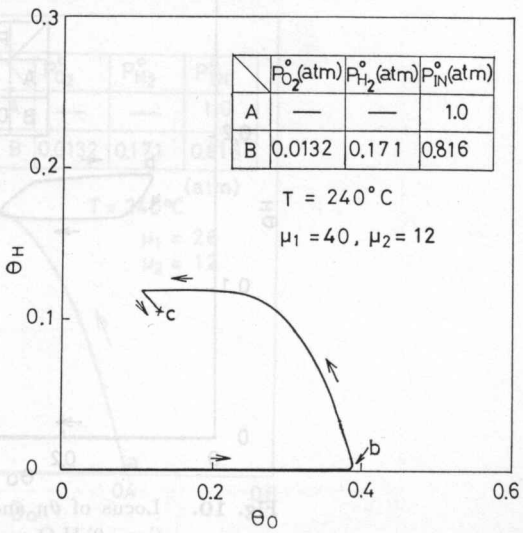

Fig. 8. Locus of θ_H and θ_O during the O_2, H_2 (inc., 0)-H_2O response in Fig. 7.

$$\frac{d\theta_H}{dt}=\frac{1}{q_m}\left\{2k_2P_{H_2}\theta_0^2-2k_{-2}\theta_H^2-2\theta_0\theta_H^2k_{30}\exp(-\mu_1\theta_0)\right\} \tag{31}$$

$$\text{where } \theta_V=1-\theta_0-\theta_H \tag{32}$$

To simulate the oscillation response, Eqns. (27)-(32) should simultaneously be solved by numerical integration, using the Runge-Kutta Gill's procedure.

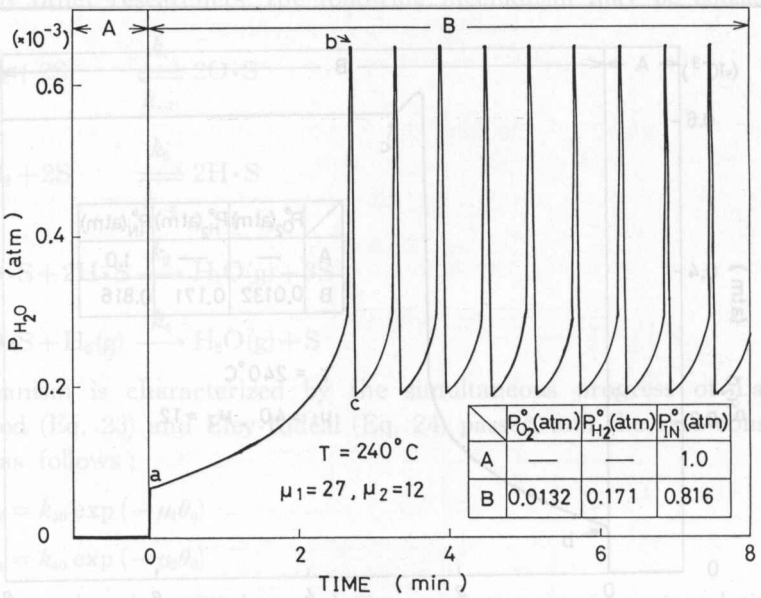

Fig. 9. Model predicted oscillation at $\mu_1=27$ and $\mu_2=12$.

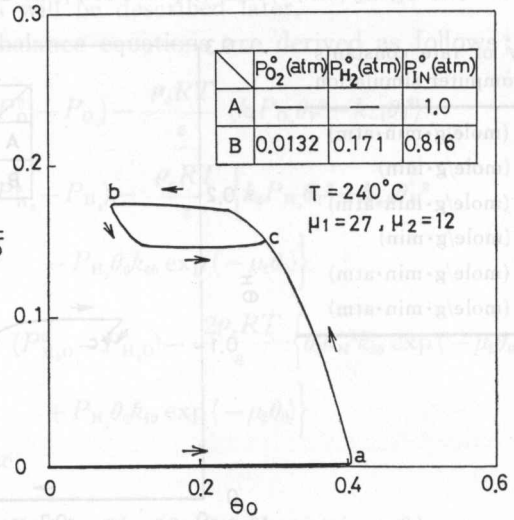

Fig. 10. Locus of θ_H and θ_O during the O_2, H_2 (inc., 0)-H_2O response in Fig. 9.

3-2. Parameter Sensitivity of μ_1 and μ_2

Qualitatively, one may try to relate the values of μ_1 and μ_2 to the degree of contribution of adsorbed oxygen to the reaction rate. Our interests are in the sensitivity of μ_1- and μ_2- values relating to the oscillation behavior of H_2O, and the reactor parameters used for the computer simulation are summarized in Table 2.

(1) Sensitivity of μ_1 under Constant Value of $\mu_2=12$

Let us consider three regions of μ_1-value: (1) region I, $\mu_1=40-38$, (2) region

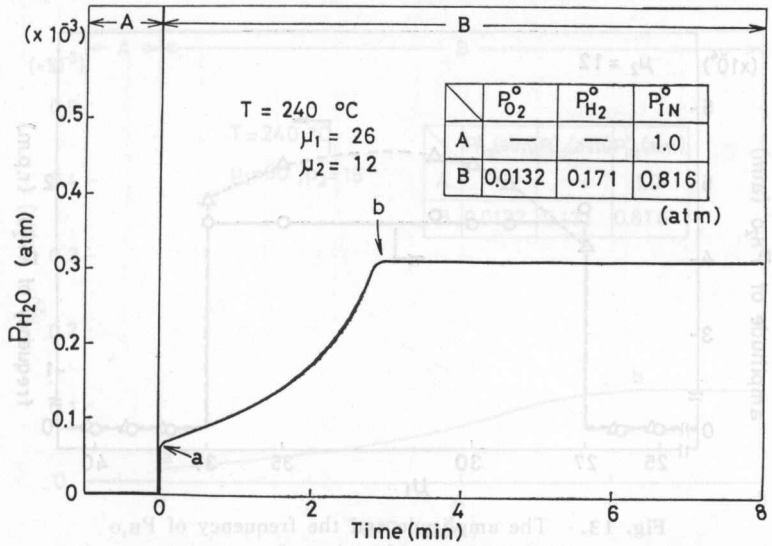

Fig. 11. The O_2, H_2 (inc., 0)-H_2O response at $\mu_1=26$ and $\mu_2=12$.

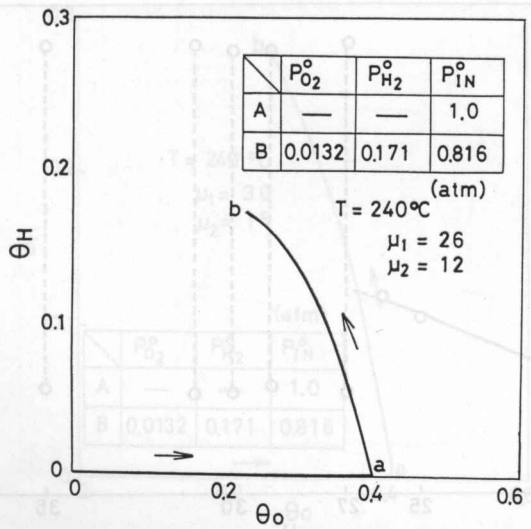

Fig. 12. Locus of θ_H and θ_O during the O_2, H_2 (inc., 0)-H_2O response in Fig. 11.

II, $\mu_1=27-37$ and (3) region III, $\mu_1=20-26$. In region I, the computer simulation is conducted by using the kinetic parameters at 240°C presented in Table 3. Here, the reverse reaction of elementary reaction (2) is assumed to be negligible. Fig. 7 illustrates a typical simulated response curves. Oscillation does not appear and the mode of the response curve exhibits a characteristic overshoot with a terrace period for about one minute. To explain the anomalous terrace period, one may be interested in the locus of the surface coverage as shown in Fig. 8. θ_0 moves up to about 0.4 with no appreciable increase of θ_H, where the changing rate of θ_0 is slow making the terrace period in Fig. 7. The θ_H then gradually

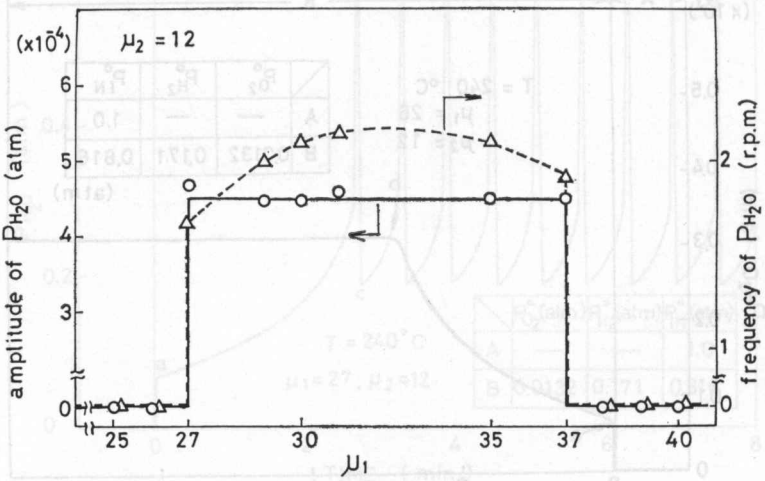

Fig. 13. The amplitude and the frequency of P_{H_2O} at $\mu_2=12$ as a function of μ_1.

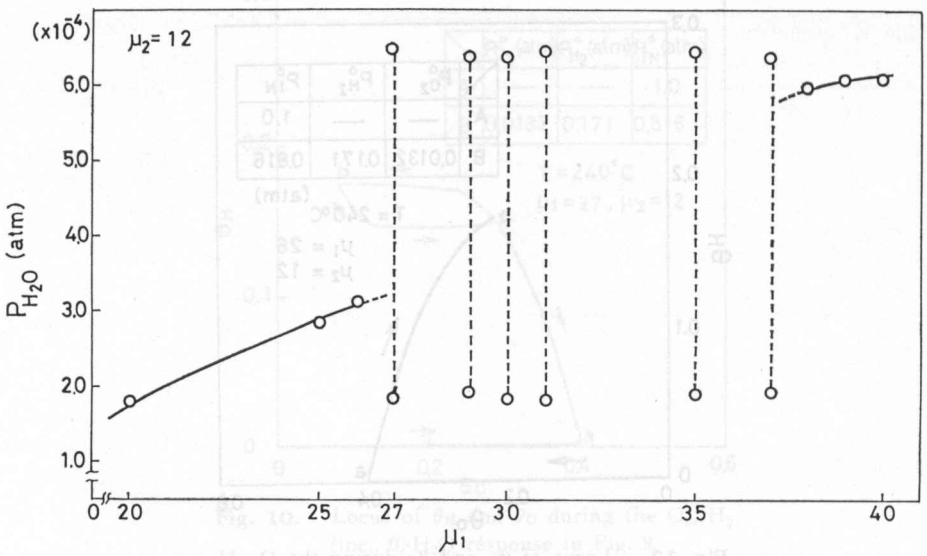

Fig. 14. Oscillation region of H_2O at $\mu_2=12$ as a function of μ_1.

increases whereas θ_0 gradually decreases. Finally, the locus is stopped at point c ($\theta_H=0.105$ and $\theta_0=0.38$).

In region II, the oscillation clearly appears as can be seen in Fig. 9. In this case, the plots of θ_H vs. θ_0 clearly make a typical closed circle which is a characteristic mode for the oscillation appearance as shown in Fig. 10. Comparing Figs. 9 and 10, points a, b and c are commonly displayed in the two figures.

In region III, Figs. 11 and 12 illustrate no oscillation indicating the typical monotonic mode of the O_2, H_2 (inc., 0)$-H_2O$ response, even though the locus of the surface coverages displays a different shape compared to that in Fig. 8.

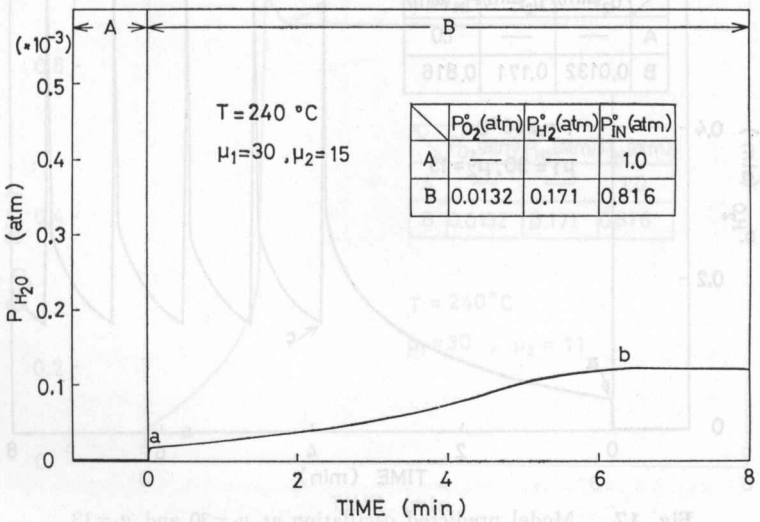

Fig. 15. The O_2, H_2 (inc., 0)-H_2O response at $\mu_1=30$ and $\mu_2=15$.

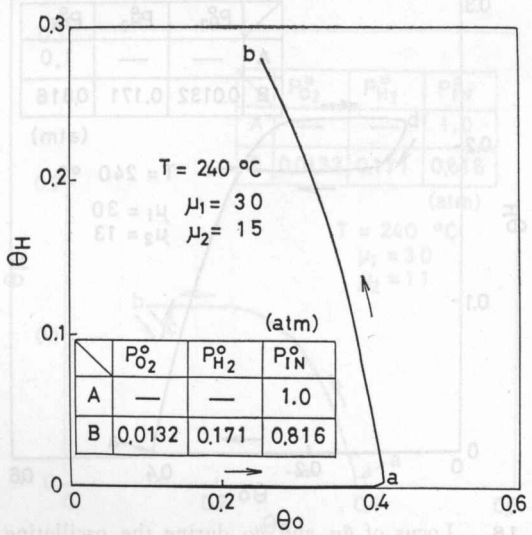

Fig. 16. Locus of θ_H and θ_O during the O_2, H_2 (inc., 0)-H_2O response in Fig. 15, a and b correspond to those in Fig. 15.

Points *a* and *b* in Fig. 11 correspond to those in Fig. 12. The characteristic mode of the response curve in Fig. 11 may be similarly explained as that in Fig. 7. Fig. 13 shows the amplitude and the frequency as a function of μ_1. As can be seen in the figure, the amplitude indicates a constant value whereas the frequency has a broad peak between $\mu_1=27$ and 37. Fig. 14 illustrates P_{H_2O}-behavior as a function of μ_1.

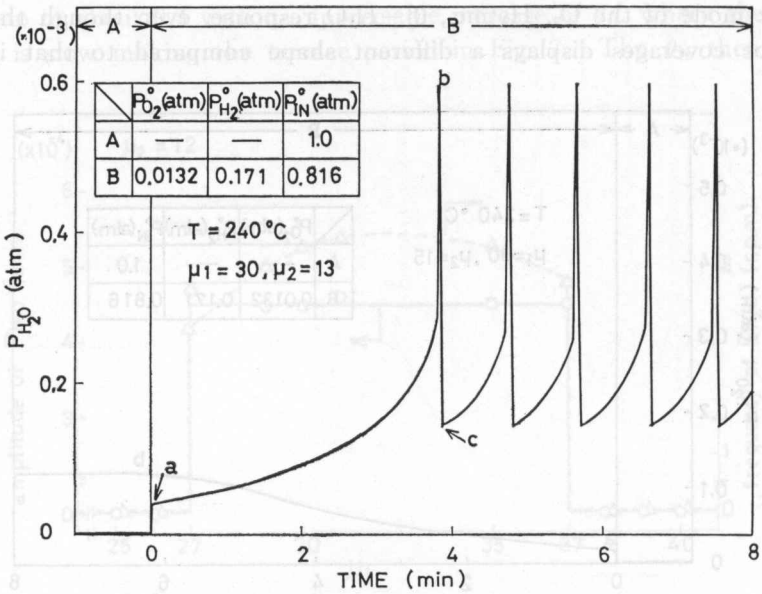

Fig. 17. Model predicted oscillation at $\mu_1=30$ and $\mu_2=13$.

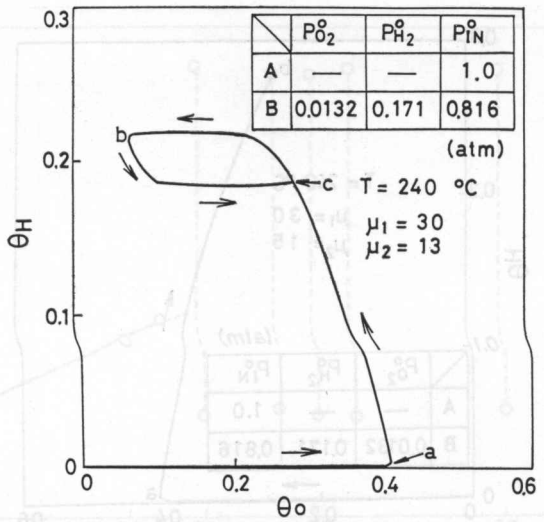

Fig. 18. Locus of θ_H and θ_O during the oscillating O_2, H_2 (inc., O)-H_2O response in Fig. 19. a, b and c correspond to those in Fig. 17.

(2) Sensitivity of μ_2 under $\mu_1=30$

A classification similar to the previous section is adopted in three regions: (1) region I, $\mu_2=14-15$, (2) region II, $\mu_2=11.5-13$ and (3) region III, $\mu_2=0-11$. The simulated results are presented in Figs. 15 and 16 for region I, Figs. 17 and 18 for region II and in Figs. 19 and 20 for region III. Oscillation appears in region II whereas regions I and III display a monotonic and an overshoot mode, respectively, with no oscillation. Comparing these results to the sensitivity of μ_1,

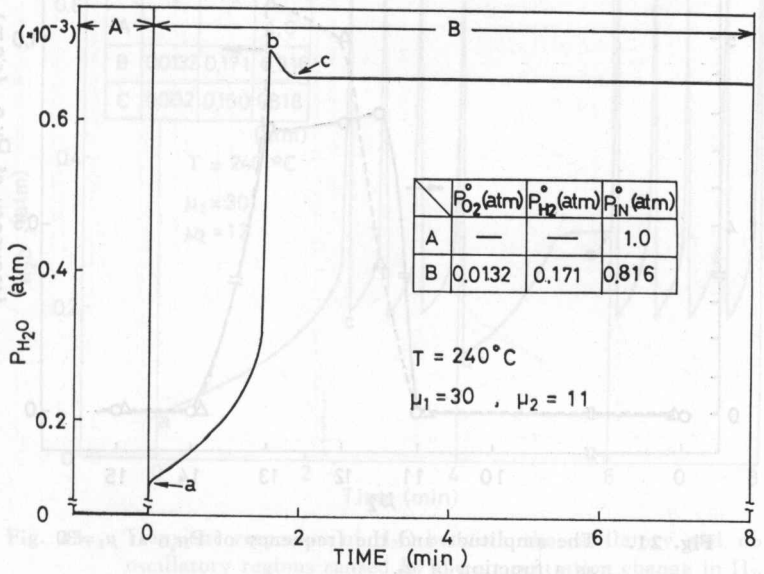

Fig. 19. The O_2, H_2 (inc., 0)-H_2O response at $\mu_1=30$ and $\mu_2=11$.

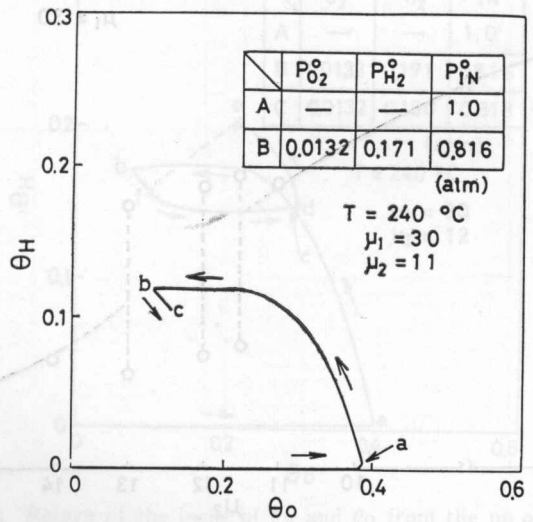

Fig. 20. Locus of θ_H and θ_O during the O_2, H_2 (inc., 0)-H_2O response in Fig. 19. a, b and c correspond to those in Fig. 19.

one may recognize that there is no appreciable change in either behaviours.

Fig. 21 displays the variation of the amplitude and the frequency as a function of μ_2. Fig. 22 illustrates the oscillating region of H_2O as a function of μ_2 at $\mu_1=30$. From these results, one may conclude the existence of a serious range of μ_2 to cause the oscillation.

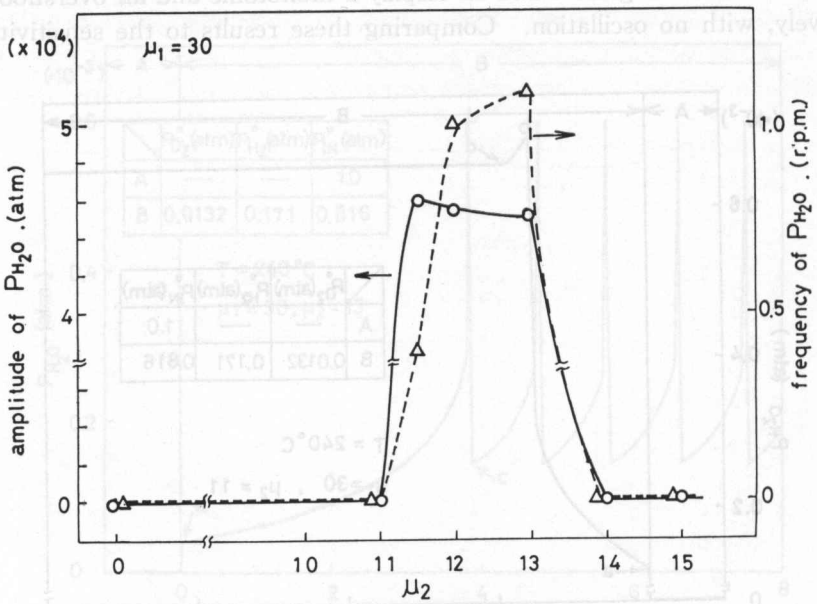

Fig. 21. The amplitude and the frequency of P_{H_2O} at $\mu_1=30$ as a function of μ_2.

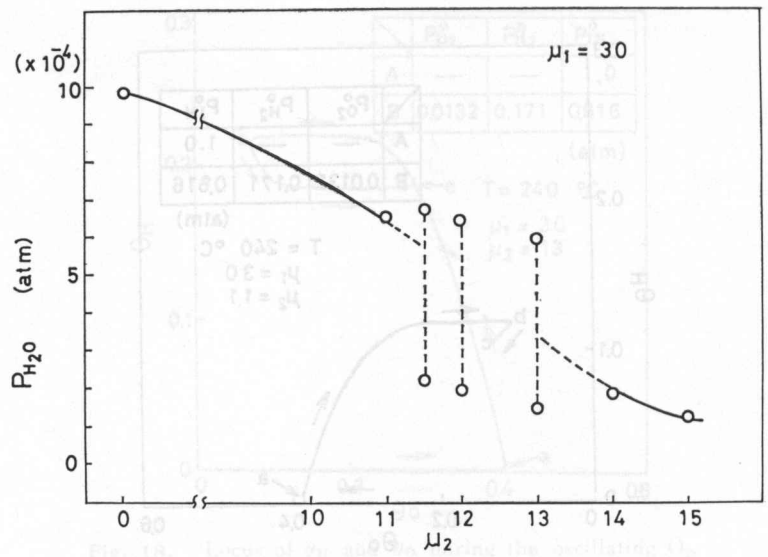

Fig. 22. Oscillation region of H_2O at $\mu_1=30$ as a function of μ_2.

3-3. Transient Oscillation Caused by the Concentration Jump

Fig. 23 illustrates the H_2-H_2O responses during the oscillation. The response curve clearly shows a characteristic transient behavior shifted from the oscillating state, according to two different concentrations of H_2, $P_{H_2}=0.171$ and $P_{H_2}=0.15$ atm. These results clearly exhibit that the oscillation states quickly shift to no

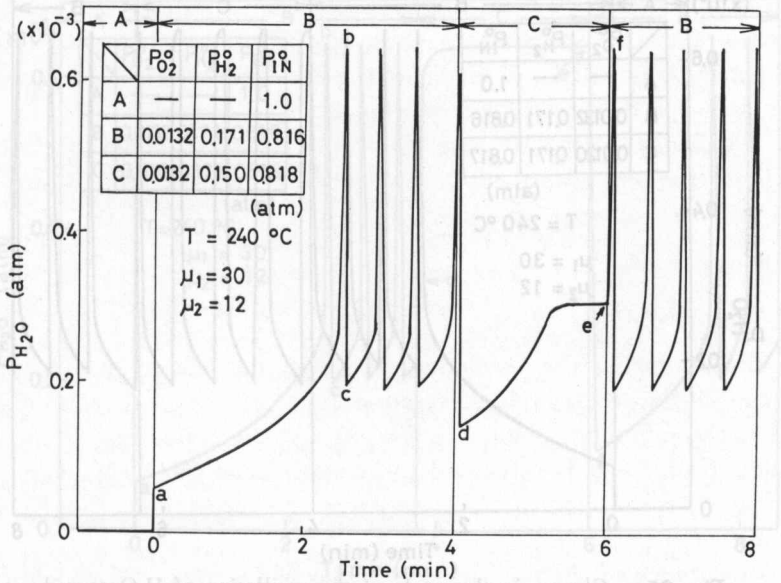

Fig. 23. Transient responses of H_2O between the oscillatory and no oscillatory regions caused by the concentration change in H_2.

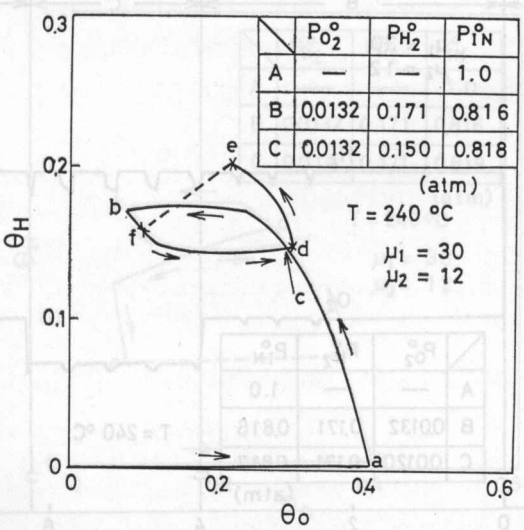

Fig. 24. Return of the locus of θ_H and θ_O from the no oscillatory region (from d to e) to the oscillatory region (circle of c, b, f). a-f correspond to those in Fig. 23.

oscillation state with no gradual change. In addition, one may recognize the concentration of H_2 higher than $P_{H_2}=0.171$ atm for the oscillation, at $P_{O_2}=0.0132$ atm. This will be changed depending on the ratio of P_{H_2} to P_{O_2}.

The locus of the surface coverages (θ_H and θ_0) is represented in Fig. 24. One may easily understand the locus of $a-f$ in Fig. 24 relating to the points of $a-f$

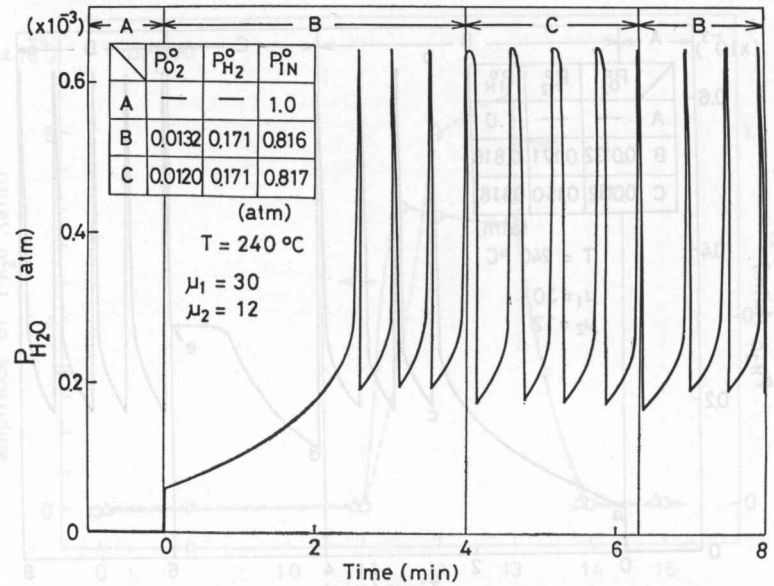

Fig. 25. Change in the mode of the oscillation of H_2O caused by the step change in the concentration of of O_2.

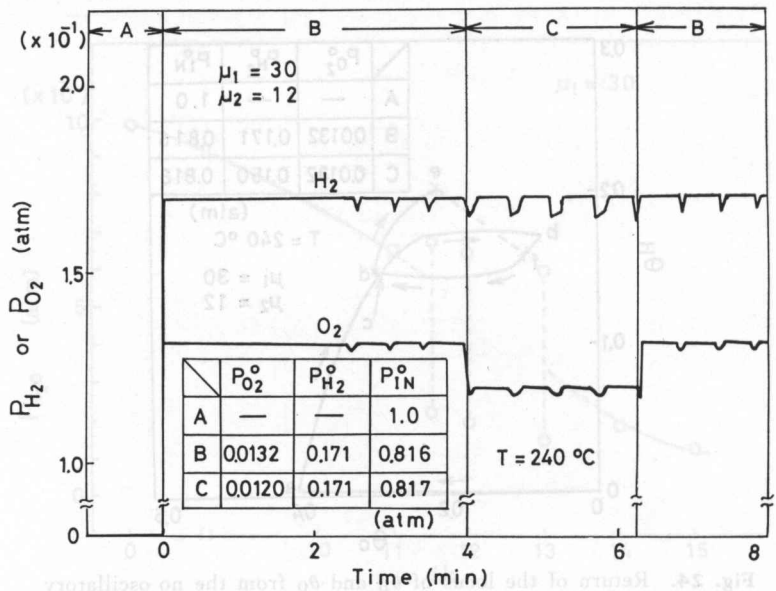

Fig. 26. Transient behavior of H_2 and O_2 during the oscillation of H_2O presented in Fig. 25.

in Fig. 23. The concentration jump of H_2 from $P_{H_2}=0.171$ to 0.15 atm drastically results in a strong deviation from the closed loop from d to e, and the opposite concentration jump gives a return from e to f displaying the oscillation.

Figs. 25 and 26 indicate the O_2–H_2O response and the O_2–H_2 and –O_2 responses, respectively. The responses in Fig. 25 show the oscillation in the two

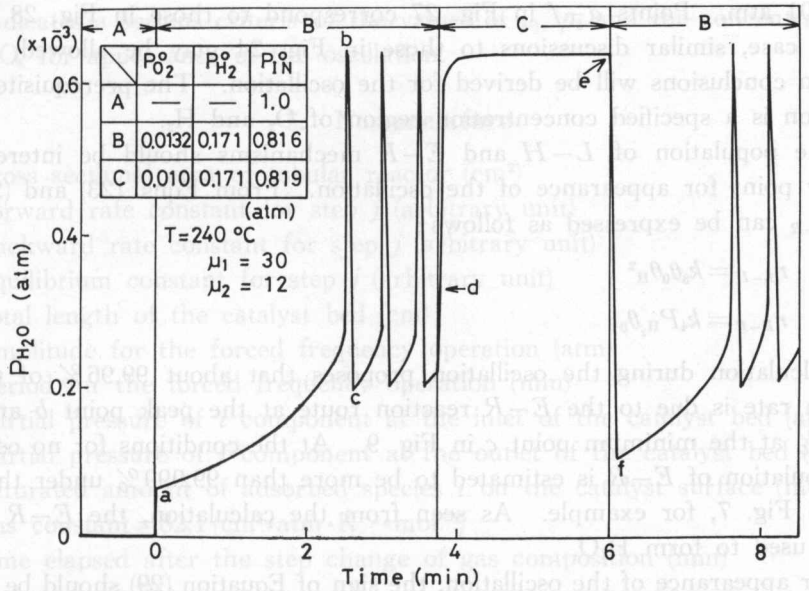

Fig. 27. Transient repsonse of H_2O between the oscillatory and no oscillatory regions.

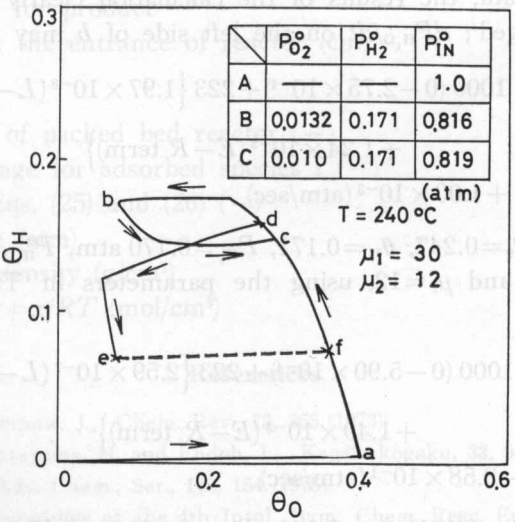

Fig. 28. Return of the locus of θ_H and θ_O from the no oscillatory region (from d to e) to the oscillatory region (circle of c, d, b).

concentrations of O_2, 0.0132 and 0.12 atm, displaying a small change in the frequency depending on the concentration. In Fig. 26, the reactants, H_2 and O_2, are slightly changed in their concentrations by the oscillation reaction, because of the differential reactor.

Figs. 27 and 28 illustrate the O_2-H_2O responses and the locus of θ_H and θ_0, respectively. The oscillation appears at $P_{O_2}=0.013$ atm whereas it disappears at $P_{O_2}=0.01$ atm. Points $a-f$ in Fig. 27 correspond to those in Fig. 28. In the present case, similar discussions to those in Fig. 24 may be allowed, and the common conclusions will be derived for the oscillation. The prerequisite for the oscillation is a specified concentration region of O_2 and H_2.

The population of $L-H$ and $E-R$ mechanisms should be interesting as the key point for appearance of the oscillation. From Eqns. (23) and (24), r_{L-H} and r_{E-R} can be expressed as follows;

$$r_{L-H}=k_3\theta_0\theta_H^2 \tag{33}$$

$$r_{E-R}=k_4P_{H_2}\theta_0 \tag{34}$$

The calculation during the oscillation proposes that about 99.96% of the total reaction rate is due to the $E-R$ reaction route at the peak point b and about 99.999% at the minimum point c in Fig. 9. At the conditions for no oscillation, the population of $E-R$ is estimated to be more than 99.999% under the steady state in Fig. 7, for example. As seen from the calculation, the $E-R$ route is mainly used to form H_2O.

For appearance of the oscillation, the sign of Equation (29) should be changed at the peak of H_2O, for example, at b in Fig. 27. One can calculate the signs of dP_{H_2O}/dt at just both sides around the peak b in Fig. 27. From the values of the simulation data, the results of the calculation clearly show that the sign of Eq. (29) is changed; dP_{H_2O}/dt on the left side of b may be calculated as

$$\begin{aligned} dP_{H_2O}/dt &= 1000\,(0-2.75\times10^{-4})+223\left\{1.97\times10^{-8}\,(L-H\text{ term})\right. \\ &\qquad \left.+1.24\times10^{-3}\,(E-R\text{ term})\right\} \\ &= +1.00\times10^{-3}\,(\text{atm/sec}) \end{aligned} \tag{35}$$

where $t=177$ sec, $\theta_0=0.247$, $\theta_H=0.171$, $P_{H_2}=0.170$ atm, $P^0_{H_2O}=0$ atm, $P_{H_2O}=2.75\times10^{-4}$ atm, $\mu_1=30$ and $\mu_2=12$, using the parameters in Tables 2 and 3. On the right side,

$$\begin{aligned} dP_{H_2O}/dt &= 1000\,(0-5.90\times10^{-4})+223\left\{2.59\times10^{-7}\,(L-H\text{ term})\right. \\ &\qquad \left.+1.49\times10^{-3}\,(E-R\text{ term})\right\} \\ &= -2.58\times10^{-1}\,(\text{atm/sec}) \end{aligned} \tag{36}$$

where $t=183$ sec, $\theta_0=0.131$, $\theta_H=0.149$, $P_{H_2}=0.168$ atm, $P^0_{H_2O}=0$ atm, and $P_{H_2O}=5.90\times10^{-4}$ atm, using the parameters in Tables 2 and 3.

4. Conclusions

The forced cyclic operation does not cause the self oscillation in heterogeneous catalysis and does not increase the efficiency to form the objective products.

The validity of Slinko's model is confirmed to be useful for the expression of the chemical oscillation in heterogeneous catalysis, in flow type reactors. The model indicates a serious criteria of the values of μ_1, μ_2 and the concentration of H_2 and O_2 for appearance of the oscillation.

5. Nomenclature

A : cross sectional area of tubular reactor (cm^2)
k_j : forward rate constant for step j (arbitrary unit)
k_{-j}: backward rate constant for step j (arbitrary unit)
K_j: equilibrium constant for step j (arbitrary unit)
L : total length of the catalyst bed (cm)
M : amplitude for the forced frequency operation (atm)
N : period for the forced frequency operation (min)
P_i : partial pressure of i component at the inlet of the catalyst bed (atm)
P_i : partial pressure of i component at the outlet of the catalyst bed (atm)
q_m : saturated amount of adsorbed species i on the catalyst surface (mol/g)
R : gas constant $=82.1\ (cm^3 \cdot atm \cdot K^{-1} \cdot mol^{-1})$
t : time elapsed after the step change of gas composition (min)
T : temperature (K)
U : superficial gas velocity (cm/min)
X : general name for reactant
Y : general name for product
Z : distance from the entrance of reactor (cm)

Greek symbols

ε : void fraction of packed bed reactor (−)
θ_i : surface coverage for adsorbed species i (−)
μ_i : constant of Eqs. (25) and (26) (−)
π : total pressure (atm)
ρ_c : catalyst bed density (g/cm^3)
ρ_M : molar density $=\pi/RT$ (mol/cm^3)

References

1) Nicols, G. and Portnow, J., Chem. Rev., **73**, 365 (1973).
2) Furusawa, T., Matsuyama, H. and Endoh, I., Kagakukogaku, **33**, 949 (1969).
3) Schmitz, R. A., Adv. Chem., Ser., **148**, 154 (1975).
4) Gilles, E. D., Proceedings of the 4th Intnl. Sym. Chem. Reac. Eng., Heidelberg (1976).
5) Takoudis, C. G., Schmidt, L. D. and Aris, R., Chem. Eng. Sci., **36**, 377 (1984).
6) Elhader, A. E. and Tsotsis, T. T., "Chemical Reaction Engineering", edited by Wei. J. and Georgakis, C., 77 (1981).

7) Puszynski, J. and Hlavacek, V., Chem. Eng. Sci., **39**, No. 4, 681 (1984).
8) Vidal, C. and Noyav, A., J. Am. Chem. Soc., **102**, 6666 (1980).
9) Hlytzavi-Stephanopoulos, M., Schmidt, L. D. and Caretta, R., J. Catal., **64**, 346 (1980).
10) Cutlip, M. and Kenney, C. N., ACS Symposium Ser., **66**, 11 (1980).
11) Kurtanjek, Z., Sheintuch, M. and Luss, D., J. Catal., **66**, 11 (1980).
12) Slinko, M. G. and Slinko, M. M., Catal. Rev. Sci. Eng., **17**, 119 (1978).
13) Van Hove, M. A., Koestner, R. J. Stair, P. C., Biberian, J. P., Kesmodel, L. L., Bartos, I. and Somarjai, G. A., **103**, 218 (1981).
14) Ertl, G., Norton, P. R. and Rustig, J., Phys. Rev. Lett., **49**, 177 (1982).
15) Bocken, O. and Wicke, E., Ber. Bunsenges. Phys. Chem., **89**, 629 (1985).
16) Sales, B. C., Turner, J. Q. and Maple, B., Sci., **114**, 381 (1982).
17) Kobayashi, M., Chem. Eng. Sci., **37**, No. 3, 393 (1982).
18) Belyaev, V. D., Slinko, M. M. and Slinko, M. G., Proceedings of the 6th Intnl. Cong. Catal., B-15, London (1976).
19) Slinko, M. G. and Slinko, M. M., Cat. Rev. Sci. Eng., **17**(1), 119 (1978).